THE CHARACTERIZATION OF A CORRODED EGYPTIAN BRONZE STATUE AND A STUDY OF THE DEGRADATION PHENOMENA

Mohamed GHONIEM *

King Saud University, College of Archaeology & Tourism Guidance,
Dep. Heritage Resources Management & Tour Guidance, Riyadh

Abstract

This paper presents the results of scientific examinations carried out on an Egyptian bronze statue discovered buried in Sais. Optical Microscopy (OM), Scanning Electron Microscopy (SEM) coupled with Energy Dispersive Spectroscopy (EDS) and X-ray Diffraction (XRD) were used to understand the corrosive morphological characteristics of the patina, to investigate the corrosion products, analyze the elementary composition of the statue and to identify the corrosive factors with effects on the alteration processes. The results indicated that the statue was made of bronze alloy, with copper as the main element, besides lead and tin. Three layers of alteration products with various composition and morphology covered the substrate of the bronze alloy. XRD results indicated that the statue was subjected to many corrosive ions such as sulfur and chloride, and buried in wet soil, rich in oxygen and carbon. This study provides useful information for the restoration and protection of the statue.

Keywords: corrosion products; patina; SEM-EDS; XRD; bronze alloy.

Introduction

Nearly all metals corrode after burial. Corrosion products can form as thin, coherent layers, or thick, disfiguring crusts that obscure the details of the object. They may protect the underlying metal or they may contain salts that cause further corrosion after the object is dug out. These corrosion products are distinctly colored, some intensely so. They represent the first visual clue to the composition of the underlying metal and reflect both the type of metal and the chemical composition of the soil.

Patina or thick corrosion crusts formed on copper, bronze or other copper alloy artifacts, may display complex products and structures. Some of those products or structural details may depend on the microstructure of the metal or the alloy, which is attacked by corrosive agents after burial. Their formation may also be influenced by a variety of growth mechanisms relating to the development and morphology of the corrosion products themselves [1, 2].

The identification of the corrosion products or characterization of the patina on archaeological bronzes is an essential requisite in order to acquire a better knowledge about the condition of ancient objects, corrosion processes and conservation treatment or preventive procedures for long-term, stable preservation.

The chemical and structural examination of the surface corrosion products grown on archaeological bronzes after burial has been a subject of study for more than a hundred years.

∗ Corresponding author: fetouhm_22@yahoo.com, P.O. Box 2627, Riyadh 12372, +966536197654

During the last decades, many researchers [3–8] have made extensive use of different analytical methods to investigate the complex structure and the composition of the bronze corrosion products (i.e., the patina) and to find a relationship between this information, the environment in which they were formed and the micro-chemical structure of the alloys.

The present paper aimed to identify the chemical composition of the corrosion layers present on an Egyptian statue stored in the Egyptian Museum, and to ascertain the structure and the morphology of the patina, as well as to determine the chemical composition of the metallic substrate or the elementary composition of the statue. This information, which can be derived from this study, may help to understand the corrosion process or the corrosive environmental conditions, to select the appropriate conservation procedures and the degree to which surface cleaning of the statue that can be carried out. Optical Microscopy, X-ray powder diffraction (XRD), scanning electron microscopy and Energy Dispersive Spectrometry (SEM-EDS) were used as analytical techniques for both characterizing and identifying the corrosion layers and to investigate the elementary composition of the statue.

Description of statue

The statue to be described (Fig.1) was discovered in Sais among a group of other bronze objects. It was temporarily inventoried with number 31/12/26/11 in the Egyptian Museum, and probably dates back to the late period (ca. 712–332 B.C.).

Fig. 1. The statue of Skhmet

It is 42 cm high, represents the goddess Sekhmet seated on a high throne. Sekhmet was a sun goddess, a fierce goddess of war, the destroyer of the enemies of Ra and Osiris. She was represented as having the head of lioness and the body of a woman, sometimes with the addition of a sun disc and uraeus serpent on her head. This impressive work that surely would have once served as a centerpiece in a temple dedicated to this mighty goddess, is characterized by increased degradation phenomena. It was covered with an extremely disfiguring crust of deposits up to a few millimetres thick and it lacked some of its parts. The statue was covered with a colored incrustation made of a variety of compounds. That incrustation, visible on the

chair or the throne, was covered with soil residues where the object had been buried. Fantastic engraved details, also present on similar statues, included whiskers around the mouth and a mane that was usually decorated with a motif resembling lotus petals. There are engravings on the throne that usually represent the symbol of the union between north and south of ancient Egypt, were hidden under this amorphous layer. Some parts from the four bottom sides of the throne, or chair were missing. The two legs lack the segment from the knees to the feet, and from the left arm only the upper part was present. The statue had fragments of the sun disk on the head and the Cobra on the forehead.

Saïs, where the statue was discovered, was the capital of Egypt during Dynasty 26 (ca. 664–525 B.C.). It was once thought to be located on the eastern Delta branch of the Nile and the ruins are to the north of the village of Sa el-Hagar.

Experimental Techniques

Optical Microscopy

The microscopical investigations were carried out using a Smart-Eye USB Digital Microscope at various magnification degrees, up to maximum 100X, for the investigation of the corrosion products characteristics and the morphology of the corrosion layer and the core of the statue, through cross-section sampling.

SEM-EDS Analyses

Scanning electron microscopy (SEM) together with energy dispersive spectrometer (EDS), was used to determine the type of alloy and the elemental composition. SEM observations were carried out on samples from the statue using the techniques of secondary and back scattering electrons. The morphology and composition of the alloy and the corrosion layers were analyzed. SEM micrographs and EDS spectra of selected specimens were obtained by using a JSM-6380 LA instrument, equipped with a Link EDS operating up to 30 kV.

X-ray Diffraction Analysis

XRD analysis was used to identify the corrosion products and soil residues covering the surface, and to understand the corrosive conditions that led to the corrosion of the object.
6 samples were taken mechanically by scraping the corroded surface gently with a very fine tungsten needle, ground to a fine powder in an agate mortar and pressed into the specimen holder, then mounted in using a Philips X-ray diffractometer type: PW1840. The operating conditions were: Cu target, 40 kV pressure, 25 mA current

Results and discussions

Microscopic examination

Both the surface of the statue and the cross-section of the alloy were investigated. Macroscopic observations allowed us to recognize the corrosion deposits and layers that completely cover the surface of the statue, their color, nature, and shape. The characterization of the surfaces by Optical and Scanning Electron Microscopy (SEM) examinations was primarily carried out without any preparation in order to keep it intact. The effects of the processes of chemical alteration on the surface of the alloy are evident in the alteration crust formed on the mineralized surface. The surface pattern appears heterogeneous and disparate at first sight optical and SEM examinations. The corrosive features such as rough, powder or compact corrosive surface, thick corrosive layer and cracks or fissures were observed. Micro photos of the surface corrosion layer (shown in figs. 2 - 6) detected different colors of the deposited layer; green to dark green, blue, and white to gray accompanied with soil traces or completely covered. This layer has different features. In some parts it is continuous, most even, and less

thick, in other parts the surface is covered in holes, where the soil residues have the color of the corrosion products and is interposed with them. The corrosion product of the green dark color, in some parts, has a shape like roes (Figs. 5), in other parts the light green colored product takes the shape of flakes, incorporated or covered with layers of transparent crystals identified as calcite (Fig. 6.).
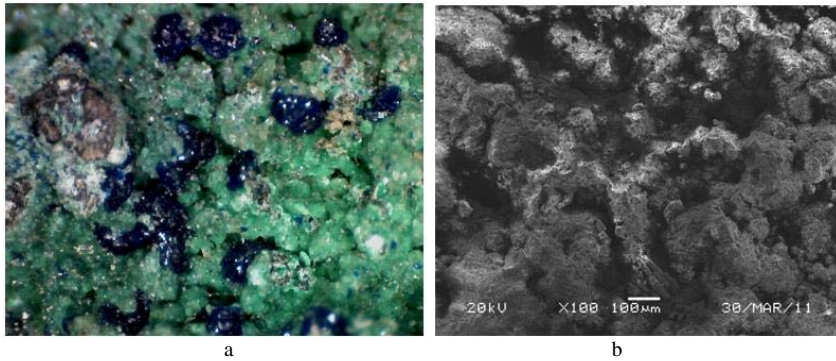

a

b

Fig. 2. The corrosion and contamination layer that has different colors on the surface:
a - optical observation (60X) and b - SEM image (x100)

a

b
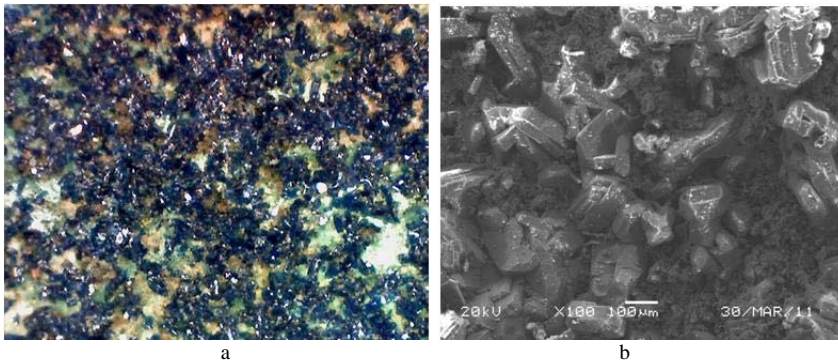
Fig. 3. The blue crystalline corrosion product sandwiches un-crystalline compound:
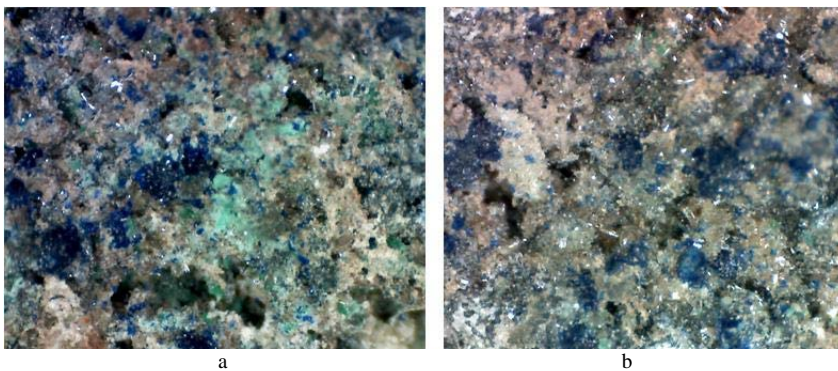a - optical observation (50X) and b - SEM image (X100)

a

b

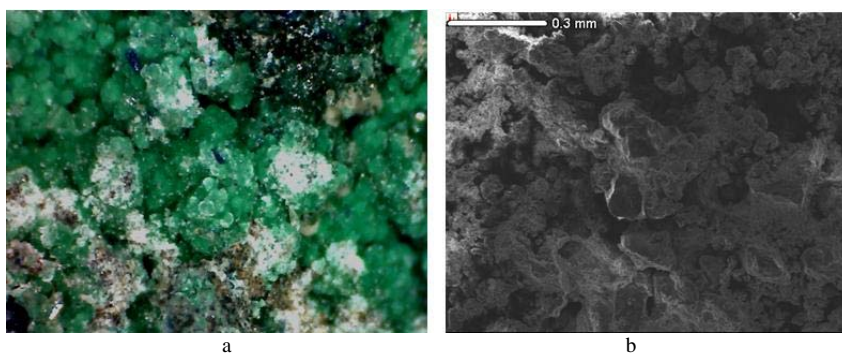**Fig. 4.** Optical observations of the outer porous layer (100X)

Fig. 5. The green corrosion product on the surface: a - optical observation (60X) and b - SEM image
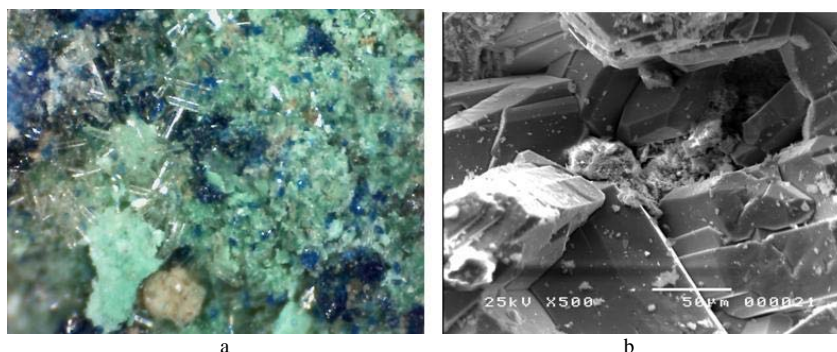

Fig. 6. The transparent crystals on the surface: a - optical observation (50X)
of the outer layer and b - SEM image (X100)

The microscopic investigation of the cross-section ascertained the strata-graphical morphology specific to most archaeological patinas of ancient bronze objects. That patina has a sandwich structure, in which the layers of the primary patina are overlapped or partially interposed with the ones of the secondary patina. The observation microphotographs (Fig. 7) show the colors, the thickness, and the layer morphology of the patina.
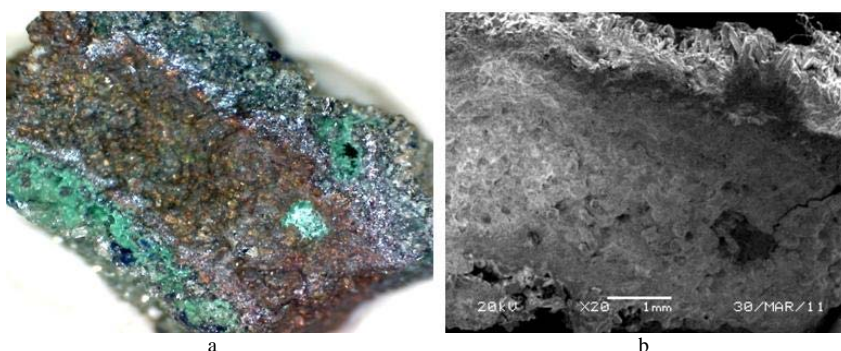

Fig. 7. The cross-section where the core of the alloy and the different features
of the corrosion layers: a - optical observation (10X), and b - SEM image (X20).

The substrate has a reddish brown color, some reddish orange lustrous crystals and has some fissures and cavities. The first internal layer of patina layers, which in contact with the alloy is irregular in shape and thickness, is sometimes not observed, coherent and has a dark brown to blackish color, concealed beneath an overlying layer of green-blue basic salts, as

corrosion products. The later layer is thicker than the previous and is covered with an outer, even thicker layer that has amorphous compounds incorporated with soil crystalline compounds and covers most of the surface (Fig. 8).
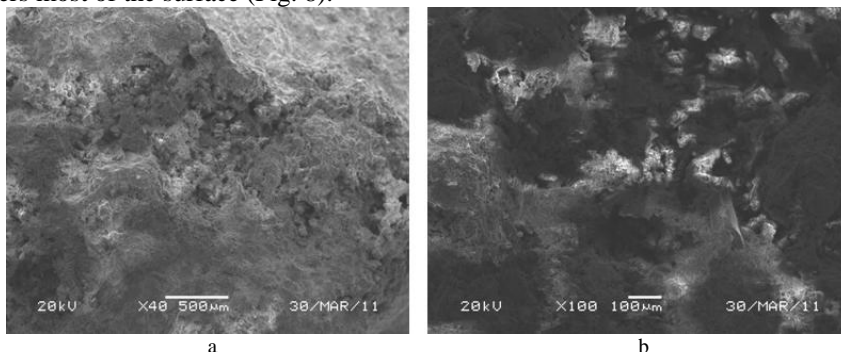

<center>a   b</center>

Fig. 8. SEM images of the outer layer, soil residues covers
the crystalline and non-crystalline corrosion products.

SEM-EDS Analysis

Six sample fragments: one cross-section sample plus 5 representative samples for the corrosion or the contamination layer were analyzed by SEM-EDS. On the same surface area where the SEM microphotography was taken, EDS microanalysis was done. From the SEM for the cross section samples, the three layers covering the substrate or the alloy's core; the internal layer, the layer of green-blue corrosion products, and the outer layer of soil relics incorporated with corrosion compounds, were identified clearly. The distribution of the chemical elements differs greatly from one area to another according to the severeness of the damage.

The results indicated the presence of some other alloy elements, apart from copper, of the original metals specific to ancient bronze, such as Pb, Sn, but also of anions resulted from corrosion and ionic exchange processes, such as carbonates, sulphates and chlorides and the contamination products based on Ca, C, S, Cl, Si, Al, Mg.

The distribution of atoms in the corrosion layers structures and the substrate, which can be deduced from the analysis, can be used a clear distinction between atoms from alloy and those resulted from corrosion and ionic exchange or the ones of contamination. The first ones (Cu, Sn, Pb) have a high percent distribution in the substrate, in the internal layer adjacent to the substrate and low concentration in the corrosion layer and the outer layer. While the percent distribution of the other ones (C, S, Cl, Si, Ca, Al, Cl, Si, Mg) is lower in the substrate, higher in the corrosion and the outer layer. The distribution of the latter chemical elements differs greatly from one area to another, according to the severeness of the damage. The definition of more precise relationships between the amounts in the elements and their distribution in this layer is not straightforward.

The elementary content revealed that the substrate or the alloy's core of the statue is bronze that contains a high percent of Cu (64.55 %,), turned to *Cuprite* in most parts where O is the minor element (18.42%), together with Pb (9.40%) and Sn (4.43%) as shown in Figure 9.

The internal layer (Fig. 10), is characterized by the presence of Cu, and Pb but less than in the alloy's core, (52.83 %) and (9.21%) respectively, and Sn (5.14%) somewhat higher than its content in the substrate, with O (18.51%), C (6.77%), Cl (4.21%), S (1.51%) and Si, Al, Fe as traces that detected by EDS as elements issued from the corrosive environment. This layer most probably consists of cuprous oxide and contains noticeable amounts of carbon, and chloride. This result has been explained by Lucey [9] considering cuprous oxide as an electrolytical membrane allowing the transport of oxygen and chloride anions inward and of cuprous ions outward. Cuprous chloride (CuCl) is also sometimes present sandwiched between the cuprous oxide layer and the substrate layer. The green-blue corrosion layer characterized by

the presence of copper in a lower content, with respect to that in the alloy's core, and various content of lead and tin, except in the whitish to gray compound sandwiched between blue crystals (Fig. 11) where tin was much higher (64.27%). In this layer, the presence of elements from the corrosive environment, mainly O, C, Ca, Cl, S, Si, was clearly detected.
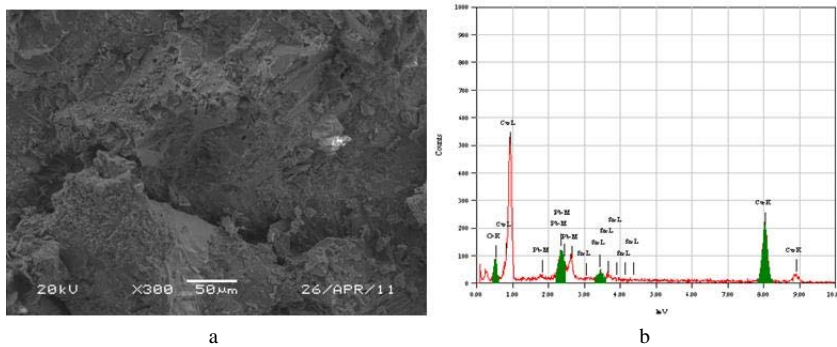

a   b

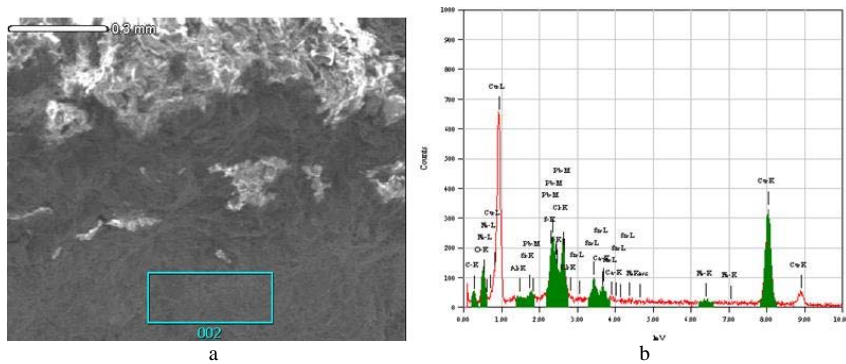**Fig. 9.** SEM and EDS analysis of the alloy's core, in which a mosaic-pattern cracking is noticeable

a   b

Fig. 10. SEM (X100) and EDS analysis of the internal layer

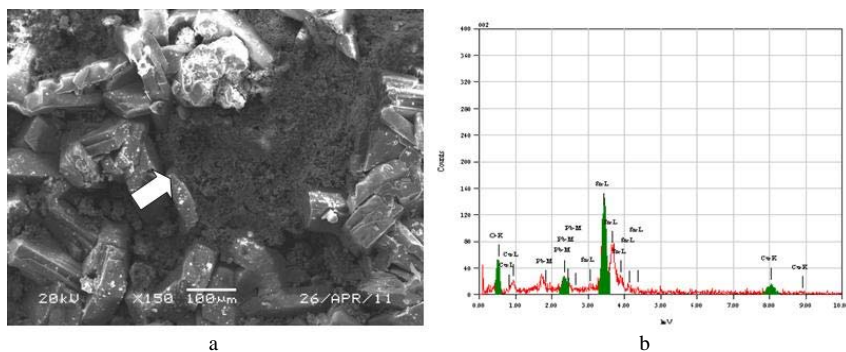a   b

Fig. 11. SEM and EDS analysis of the sandwiched compound between blue crystals

Analysis of the two samples of green corrosion product (Figs. 12 and 13) detected the presence of Cu as the major element (41.34% and 55.82%), O (24.39 -17.81%), C (14.32 - 15.19%), Si (14.32 - 2.19%), Cl (5.23 - 7.13%) respectively in the two samples, in addition to Al, Fe, Mg, Ca and S as traces elements. This indicates that this layer of green corrosion product of copper carbonate that confirmed by XRD analysis.
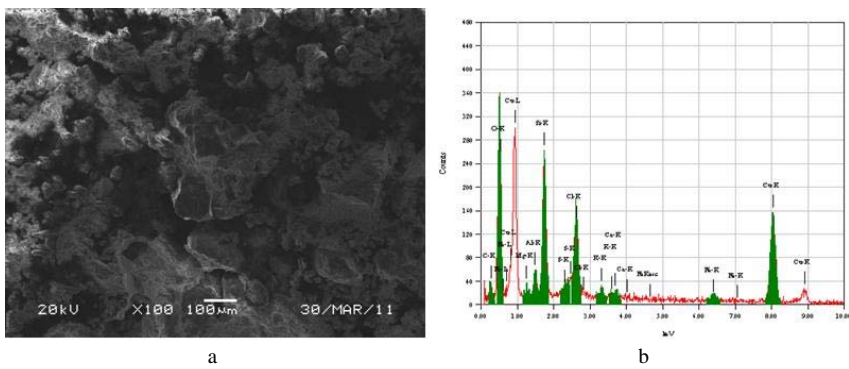
a   b

Fig. 12. SEM and EDS analysis of the green corrosion product
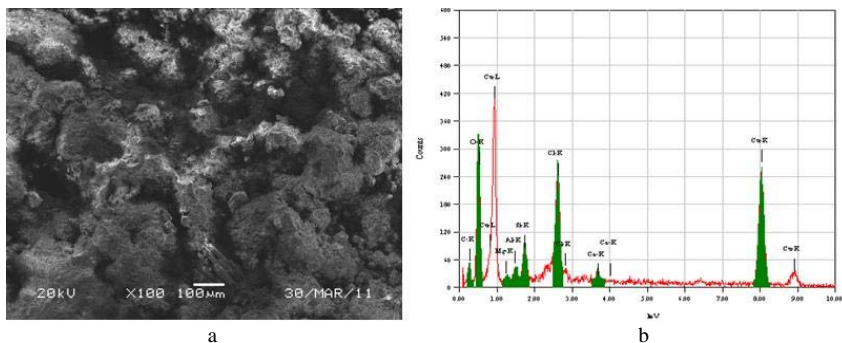

a   b

Fig. 13. SEM and EDS analysis of the greenish corrosion product

Analysis of the blue color corrosion layer detected the presence of copper as the major element (47.28%), C (31.10%), O (17.08%), and Si (4.54%) (Fig. 14). While the gray sandwiched corrosion product between the blue crystals has Sn as the major element (64.27%), in addition to O (19.91%), Pb (8.04%), and Cu (7.78%). This is probably because of the deposition of tin oxide corrosion product (Fig. 11).
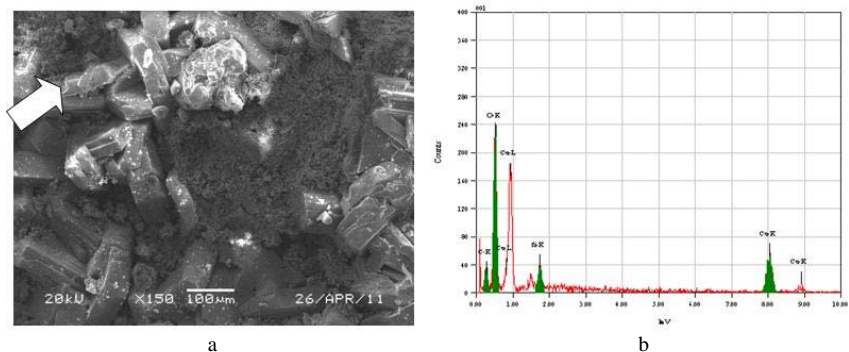

a   b

Fig. 14. SEM and EDS analysis of blue color corrosion

The greenish blue corrosion product that covered some parts of the statue characterized with the presence of copper in a less content (31.18%), C (24.97%), O (17.23%), Pb (11.24%), Ca (6.16%), Cl (1.42 %), Sn (0.25 %), besides Mg, Al, Si, and Fe as traces.(Fig. 14).

The outer layer is rich in soil elements and has the least content of copper and tin where there is not lead. EDS analysis detected the presence of C (29.82%), O (24.38%), Ca (23.16%), Si (3.93%), S (2.68%), Cl (1.52%), P (1.74%), Al (1.23%), Mg (0.86%), whereas Cu was

(8.60%), and Sn was (2.06%) (Fig. 15). Most of these elements were confirmed as carbonates, sulphides, chlorides and oxides by XRD analysis.
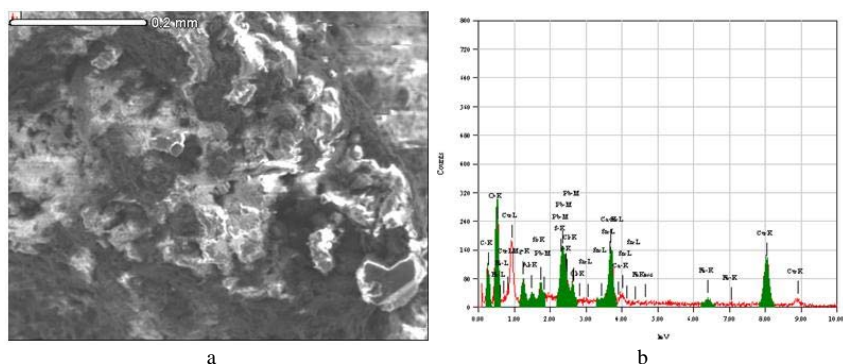

a   b

Fig. 15. SEM and EDS analysis of the greenish blue corrosion product

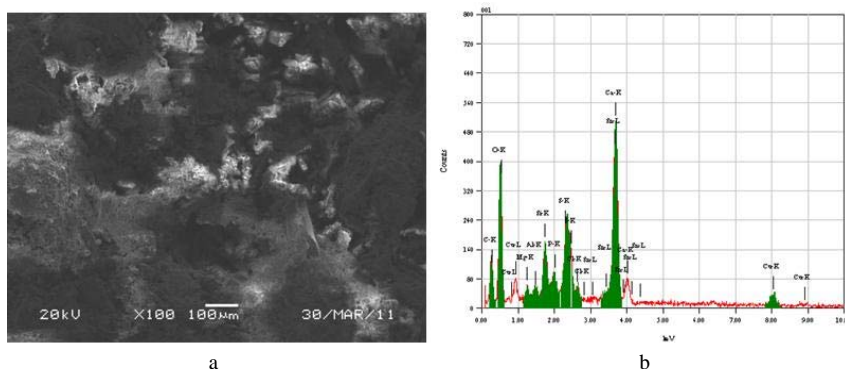a   b

Fig. 16. SEM and EDS analysis of the outer layer rich in soil elements

From the above results, it is considered that the initial step of the corrosion process is the dissolution of the alloy surface after it was buried into the soil despite the fact that some corrosion history of the object may have existed before its burial. Depending on the rate and the homogeneity of the attack, the alloy oxidation will lead to the formation of different surface films, a low dissolution rate of copper and tin will lead to a protective surface film, allowing the formation of an enriched tin layer associated with the selective dissolution of copper. While at high dissolution rates, copper and tin dissolution should occur without formation of protective layers. In this last case, due to the higher concentration of copper ions in the corrosive medium, deposition of copper products may then rapidly occur without strong protective effect, allowing a multilayer structure to develop that consist of the compounds of the present anions in the surrounded environment.

XRD Analysis
The X-ray powder diffraction patterns shown in Figures 17-19 are representative of the patterns obtained from 6 samples of different corrosion products covering the statue. The detected corrosion compounds were listed in table No. 1. Results revealed that the main constituents of the surface layer of the patina are green colored copper (II) compounds incorporated with soil components covering a red cuprous oxide layer in contact with the metal core of the alloy. Most of these compounds related to copper, in addition to lead (*Cerussite*, *Plattnerite* and lead oxide chloride hydrate) and tin (*Cassiterite*), that detected by EDS as the

main elements of the alloy. These compounds are mainly of oxides, carbonates, chlorides, besides sulphides, sulphates.

Cupreous oxide Cu_2O (Cuprite) was detected as the major compound in samples No. 1 (Fig. 17a), and No. 2 (Fig. 17b), a minor compound in sample No. 4, and as a trace in sample No. 5, and sample No. 6. This confirmed that *Cuprite*, the first and most widely occurring alteration mineral of ancient copper and its alloys, formed during burial, underground before excavation, as a result of exposure to oxygen or moist air [10]. The presence of metallic copper in the *Cuprite* patina in sample No. 1 and No. 2 may be from the dissolution of *Cuprite* formed during burial. The *Cuprite* layers that develop as a result of subsequent corrosion may also be subject to reductive processes, with formation in some areas of redeposited copper. *Cuprite* is known to play a decisive role in the protectiveness of corrosion layers on copper. But increase in oxygen pressure breaks its conformity and provoke its dissolution resulting in formation of flaws, through them Carbon dioxide and other various gases and ions are able to penetrate that favor local cell activity leading to amassment of basic copper corrosion carbonates, chlorides, and sulphates.

Malachite - $CuCO_3.Cu(OH)_2$ was identified as the major corrosion product in sample No. 3 (Fig. 18a) representing a dark green layer, and as a minor compound in sample No.5 (Fig. 19a) and as a trace in sample No.1. While *Azurite* - $Cu_3(CO_3)_2(OH)_2$ that has a similar composition to malachite, was less than *Malachite* as it was identified only in sample No. 4 (Fig. 18b) representing blue corrosion product. Its is most likely that malachite and azurite are formed by contact with soil water charged with carbon dioxide or carbonic acid in poorly aerated soil [11]. Azurite as a patina mineral has been observed only on copper alloys that have been excavated from soil. And it is formed only from solutions with high concentration of hydrogen carbonate ion (HCO_3^-). The presence of azurite indicates that the object corroded in the presence of elevated hydrogen carbonate activity, which usually results from the dissolution of calcium carbonate $CaCO_3$ by CO_2-rich water [12]. And this is the same condition that helps in forming lead carbonate *Cerussite* - $PbCO_3$, which identified in samples No.5 (Fig. 19a) and No.6 (Fig. 19b), as a result of reaction of lead in the alloy with carbon dioxide. The rarity of Azurite in corrosion products, compared to malachite, is due to its lower stability than malachite and its ability to be converted to malachite in the presence of moisture through loss of carbon dioxide. [13].

Calcite or calcium carbonate $CaCO_3$ was found in sample No.6 (Fig. 19b), representing soil relics, incorporated with corrosion products and sample No.1. This confirmed the EDS analysis of the outer layer rich in soil elements C, Ca and oxygen. However, it can't be deduced that the burial soil was calcareous soil as *Quartz* (SiO_2), the main component of sandy soil, was detected in samples No.1, 4, 5, and 6. Also high *Quartz* was identified in sample No. 6. This means that the burial soil is most likely a mixture of sand and lime.

Atacamite - $Cu_2(OH)_3Cl$ was identified as the major compound in samples 2 (Fig. 17b), 4 (Fig. 18b), and as the main compound associated with *Paratacamite* - $Cu_2CO_3(OH)_2$, representing the pale green corrosion product. The latter compound was found also as a minor compound in sample No. 5 and as a trace amount in sample No. 1. *Atacamite* was found as the second component in the reddish brown *Cuprite* sample No. 2, this indicates that *Cuprite* is the inner primary layer that followed by the overlying Cooper (II) chlorides or may be a secondary compound resulting from hydrolysis of cuprous chloride - CuCl (*Nantokite*) when exposed to moisture or moist air. These compounds (*Atacamite and Paratacamite*) are formed as a result of exposure to a long contact with saline soil richer with chloride content at high moisture level. It is known that the Egyptian soil is rich in sodium chloride that is highly reactive toward copper and its alloys. They may occur as original corrosion products or as transformation products from CuCl (*Nantokite*) that can be oxidizes to red cuprous oxide – Cu_2O (*Cuprite*) and bright green basic cupric chloride (*Atacamite*). The latter often is altered to a paler green powdery

product (Paratacamite) identical in chemical composition but differing in crystal form. (hexagonal) from Atacamite (orthorhombic) [11].
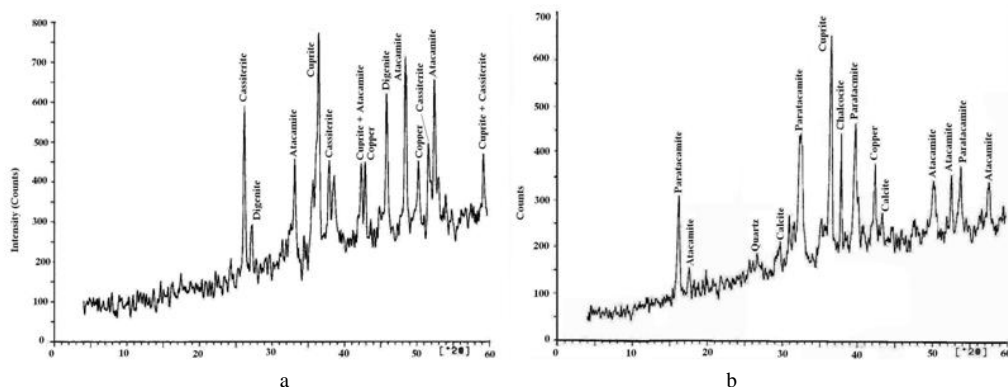

Fig. 17. XRD pattern representing the patina of the surface: a – sample 1, b – sample 2
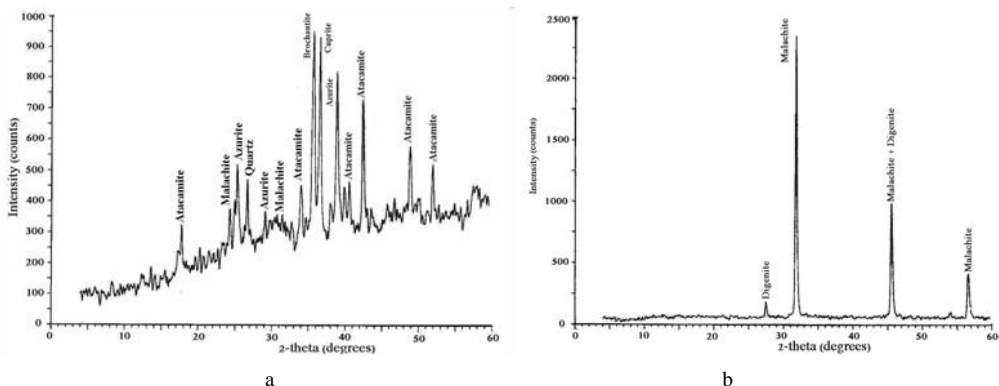

Fig. 18. XRD pattern of: a - sample 3 representing the dark green corrosion product;
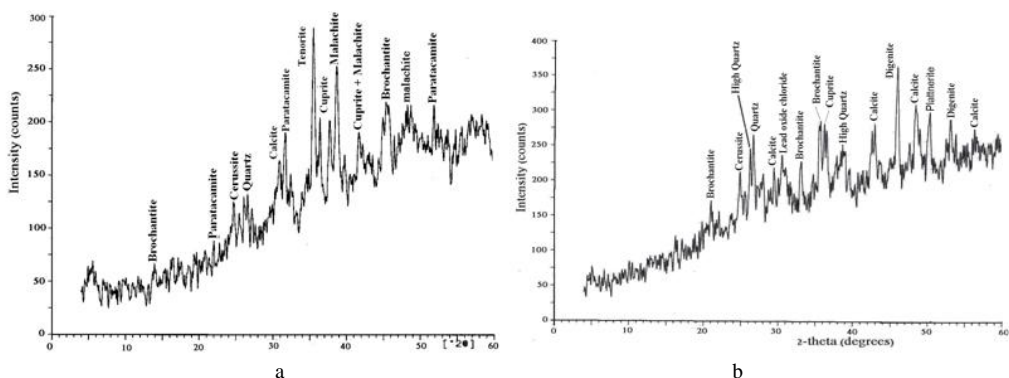b - sample 4 representing greenish blue corrosion product

Fig. 19. XRD pattern of: a - sample 5 representing the dark green corrosion product;
b - sample 6 representing the soil residues incorporated with corrosion products.

The green basic copper sulphate - $Cu_4SO_4(OH)_6$ (*Brochantite*) found as a major compound in samples No.4 (Fig. 18b) and No.5 (Fig. 19a), that usually reported on bronze artifacts exposed to sulfur-bearing waters or atmospheres. It is seldom to be found on copper alloy objects buried in soil. Also copper sulphides - Cu_2S (*Chalcocite*) and Cu_9S_5 (*Digenite*) were detected. The first one in sample No.1, and the second in samples No.2, 3, 6. This is probably as a result of burial oxygenated conditions, where hydrogen sulphide is evolved as a consequence of bacterial reduction of sulphates that utilize the oxygen for oxidative enzymatic activity from the microfauna present in the humus found in the soil sediments. Under this condition, sulfide ions are produced, thus giving rise to the formation of copper sulfides via the interaction with copper ions [13].

Cassiterite, resulted from the segregation and diffusion processes in the inferior layers, was detected in sample No. 2 and associated with *Azurite* in sample No. 4 that represent the bluish corrosion product, that shows a similar result to the analysis by SEM-EDS. Lead compounds, such as PbO_2 (sample No. 2, 3, 6), $PbCO_3$ (sample No. 5, 6), and $Pb_4O_3Cl_2 \cdot xH_2O$ (sample No. 6) were detected. These compounds resulted from the selective dissolution of lead, the second main element of the alloy, by reaction with the surrounded corrosive ions such as oxygen, carbon and chloride.

Table 1. Identified corrosion compounds by XRD analysis.

Corrosion product	Formula	Index no.
Atacamite	$Cu_2(OH)_3Cl$	25-269
Azurite	$Cu_3(CO_3)_2(OH)_2$	11-682
Brochantite	$Cu_4SO_4(OH)_6$	13-398
Calcite	$CaCO_3$	5-586
Cassiterite	SnO_2	2-1337
Cerussite	$PbCO_3$	5-417
Chalcocite	Cu_2S	12-227
Copper	Cu	1-1241
Cuprite	Cu_2O	5-667
Digenite	Cu_9S_5	9-46
High Quartz	SiO_2	11-252
Lead oxide chloride hydrate	$Pb_4O_3Cl_2 \cdot xH_2O$	6-404
Malachite	$Cu_2CO_3(OH)_2$	10-399
Paratacamite	$Cu_2(OH)_3Cl$	15-694
Plattnerite	PbO_2	8-185
Quartz	SiO_2	5490

Conclusions

From different viewpoints discussed in this paper, the examination under optical and SEM conditions allowed us to identify the nature of the alloy, characterized by the presence of cracks or fissures and cavities most probably representing selective corrosion of Pb islands.

The examination of the cross-sectioned patina revealed its complex structure and allowed the identification of three different and irregular layers of corrosion products. First, a thin internal layer, with a dark reddish brown to blackish color, followed by a thick layer of greenish, bluish and gray corrosion products. The latter covered with an outer layer of soil traces incorporated with colored corrosion products. These layers are characterized by different chemical composition with variable content of the alloy elements (Cu, Sn and Pb) and elements coming from the soil such as P, Cl, Al, Ca and Fe.

EDS analysis indicated that the statue was made of bronze alloy, where copper is the major element, in addition to lead and tin in a lower quantity. Lead is sometimes added to act as an internal lubricant, it makes the alloy easier to cast and process. Since ancient times, bronze has been the preferred material for casting statues and other decorative artifacts because it reproduces every detail of the mold and because of its high corrosion resistance, which ensured

that the statue will last. The presence of oxygen, as a minor element and in a content, more than lead and tin, in the core of the alloy indicated that cooper was transferred to cuprous oxide *Cuprite*. Copper content decreased from the core to the corrosion layers to be the least content in the outer layer. While the content of lead or tin was various. The first internal layer was identified as *Cuprite*, the second colored layer was composed of different corrosion compounds, such as, oxides, carbonate, sulphate, sulphides, and chlorides of copper, lead, and tin that were detected by XRD and EDS. While the third layer was composed of corrosion products and soil compounds, *Calcite* and *Quartz.*

The XRD results indicate an interaction between soil constituents, such as Cl, Ca, S, C in the presence of oxygen, carbon dioxide and water, with the bronze components which produces variety of corrosion products..

The green corrosion product is constituted of alkaline compounds of copper such as hydroxycarbonates (*Malachite*), hydroxychlorides (*Paratacamite or Atacamite*), or sulphides (*Chalcocite and Covellite*). The blue and bluish green corrosion product is identified as cooper hydroxycarbonate (*Azurite*) and copper hydroxysulphate (*Brochantite*). All the identified corrosion compounds by XRD confirm the metallic composition of the statue that detected by EDS, the corrosive factors resulted in its deterioration and how it was in bad burial conditions, where chloride, sulfur corrosive ions and carbon dioxide, oxygen, and water were predominating.

Acknowledgements

References

[1]   D. Scott, *Periodic corrosion phenomena in bronze antiquities*, **Studies in Conservation, 30,** 1985, pp. 49-57.
[2]   I. Sandu, M. Quaranta, C. Bejinariu, I.G. Sandu, D. Luca, A.V. Sandu, *Study on the specific effects of corrosion processes on ancient bronze artifacts*, **Annals of "Dunãrea de Jos" University of Galati, Fasc. IX. Metallurgy and Materials Science, 1,** 2007, p. 64-63.
[3]   W.A. Oddy, N.D. Meeks, *Unusual phenomena in the corrosion of ancient bronzes*, **Science and technology in the service of conservation** (ed. N. S.Brommelle and G. Thomson). International Institute for Conservation of Historic and Artistic Works, London, 1982, pp.119–124.
[4]   D.A. Scott, *Bronze disease: a review of some chemical problems and the role of relative humidity*, **Journal of the American Institute for Conservation, 29**, 1990, pp. 193-206.
[5]   D. Thickett, M. Odlyha, *Note on the identification of an unusual pale blue corrosion product from Egyptian copper alloy artifacts*, **Studies in Conservation**, **45**, 1, 2000, pp. 63-67.
[6]   K. Trentelman, L. Stodulski, D. Scott, M. Back, S. Stock, D. Strahan, A.R. Drews, A. O'Neill, W.H. Weber, A.E. Chen, S.J. Garrett, *The Characterization of a New Pale Blue Corrosion Product Found on Copper Alloy Artifacts*, **Studies in Conservation**, **47**, 4, 2002, pp. 217-227.
[7]   G.M. Ingo, E. Angelini, T. de Caro, G. Bultrini, I. Calliari, *Combined use of GDOES, SEM-EDS, XRD and OM for the microchemical study of the corrosion products on*

archaeological bronzes, **Applied Physics. A, Materials Science & Processing**, **79**, 2004, pp. 199-204.

[8] F. Gallese, G. Laguzzi, L. Luvidi, V. Ferrari, S. Takacs, G. Venturi, P. Cesa, *Comparative investigation into the corrosion of different bronze alloys suitable for outdoor* sculptures, **Corrosion Science, 50,** 2008, pp. 954–961.

[9] V.F. Lucey, *Development leading to the present understanding of the mechanism of pitting corrosion of copper,* **British Corrosion Journal, 7,** 1972, p. 36-41.

[10] J. Wang, C. Xu, G. Lu, *Formation processes of CuCl and regenerated Cu crystals on bronze surfaces in neutral and acidic media*, **Applied Surface Science, 252,** 2006 pp. 6294–6303.

[11] R.J. Gettens, *Mineral alteration products of ancient metal objects*, **Recent Advances in Conservation**, London, Butterworths, 1963, p.90.

[12] W.A. Franke, M. Mircea, *Plutarch's report on the blue patina of bronze statues at Delphi: A scientific explanation*, **Journal of the American Institute for Conservation, 44, 2,** 2005, pp.103-116.

[13] D.A. Scott, **Copper and Bronze in Art, Corrosion, Colorants, Conservation**, Getty Conservation Institute, Los Angeles, USA, 2002, p. 108, 124.